Original Research

Exploring the Potential of Phase Change Material for Thermal Energy Storage in Building Envelopes

Zachary Brozzesi [1], Darson Dezheng Li [2], Ann Lee [1, *]

1. School of Engineering, Macquarie University, NSW 2109, Australia; E-Mails: zachary.brozzesi@students.mq.edu.au; ann.lee@mq.edu.au
2. School of Mechanical and Manufacturing Engineering, The University of New South Wales, NSW 2052, Australia; E-Mail: darson.li@unsw.edu.au

* **Correspondence:** Ann Lee; E-Mail: ann.lee@mq.edu.au

Academic Editor: Islam Md Rizwanul Fattah

Special Issue: Environmental Burden Reduction Through Sustainable Energy

Abstract

Buildings, with their significant energy consumption, pose a pressing concern for the future. Inadequate heating, ventilation, and air-conditioning (HVAC) systems further exacerbate thermal management difficulties and energy requirements. To address these challenges, Phase Change Materials (PCMs) offer valuable potential for sustainable energy reduction within the building sector, leveraging passive cooling and heating techniques. Numerical study has been conducted to explore the impact of embedding PCM within the building envelope on energy efficiency and thermal performance. The results reveal that PCM integration significantly reduces temperatures across all sections compared to scenarios without PCM. By passively absorbing and storing heat energy during phase change, PCM mitigates heat transfer through convection and conduction, leading to improved energy efficiency and reduced power consumption for cooling and heating purposes. Within the first 2 hours, the PCM achieves 50% of its average melting process, followed by a gradual decrease in the melting rate. It takes approximately 6 hours for the PCM to completely melt. As the PCM undergoes the melting process, the system's entropy values increase, reflecting an increase in disorder.

At the tip of the building, the entropy value reaches 130 K/kg·K, which is more than three times the initial value. The integration of PCM in building envelopes shows promising potential for enhancing energy efficiency, thermal comfort, and durability. Future research should focus on optimizing PCM placement and configuration to maximize its benefits in diverse building designs and climatic conditions.

Keywords

Phase change material; thermal energy storage; building envelopes; melting; heating; sustainable energy reduction

1. Introduction

Thermal comfort, which refers to an individual's perception of their body temperature, is a crucial aspect of indoor environmental quality that has a significant impact on workplace productivity and health and safety [1]. Heating, Ventilation, and Air-Conditioning (HVAC) systems are widely used to improve thermal comfort, but they consume a substantial amount of energy, accounting for up to 40% of energy usage in office buildings and 70% in residential homes in Australia [2]. The depletion of energy supplies and environmental concerns such as excessive CO_2 emissions, global warming, air pollution, and ecosystem degradation have made energy consumption in buildings a pressing issue worldwide [3, 4]. To address this problem, sustainable buildings have been developed as a holistic, integrated, multidisciplinary approach to creating environmentally responsible infrastructure systems [5].

One sustainable building solution is the utilisation of Phase Change Materials (PCMs), which have a large thermal mass and latent thermal storage that enables buildings to maintain acceptable temperatures through melting and solidification behaviours [3].

PCMs have been utilized to enhance a building's thermal performance by maintaining thermal comfort and reducing energy consumption [6]. Incorporating PCMs into a building can achieve greater heat storage capacity through the absorption of solar radiation and the storage of latent heat during phase transitions [6]. PCMs have shown promise in various heat transfer and energy storage applications, including solar, thermal storage, HVAC, and heat sinks related to electrical products and photovoltaic modules [7]. PCMs can be added to buildings at any stage of their lifespan, including new construction or renovation projects [7]. They can be incorporated into building components such as walls, roofs, and facades as passive systems or used as active systems in heat and cold storage units [8].

There are several methods for incorporating PCMs into buildings, including direct impregnation/incorporation, immersion, shape-stabilization, macro-encapsulation, microencapsulation, and form-stabilization [7]. Direct impregnation is the easiest and most economical method, but it has limitations, such as potential leakage during the melting phase of the PCM and a decline in the mechanical properties of the building material as a result of the manufacturing process [7]. Immersion can cause leakage, incompatibility problems, and long-term deficiencies [3]. Shape-stabilization, form-stabilization, and encapsulation techniques offer

advantages such as increased shelf life, improved thermophysical properties, and prevention of leakage [3].

According to a report [9], windows contribute up to 60% of a building's total energy consumption. In line with this concern, Yang et al. [9] conducted a study investigating the effectiveness of double-glazed windows containing nanoparticle-enhanced PCM. The outcomes of their research revealed a notable reduction in energy consumption within a hybrid nano-PCM glazed window, showcasing promising and encouraging results.

As demonstrated by Uludaş et al. [10], analyzing a scenario using PCM for thermal enhancement and its effect on a building's thermal inertia within sunspaces, results indicate that proper optimization can lead to a 20% reduction in energy consumption for buildings. Incorporating PCMs into buildings has been shown to improve thermal inertia, reducing energy consumption and costs associated with heating and cooling systems [7]. Additionally, it has been suggested that the use of PCMs may improve indoor air quality and acoustic comfort in buildings [1, 8]. Studies have shown that the use of PCMs can result in significant reductions in energy consumption and CO_2 emissions in buildings [7]. However, further research is needed to investigate the long-term performance and economic viability of PCM-based systems in various building applications. In the study conducted by Liu et al. [11], the thickness of PCMs was explored for its effect on the thermal performance of building structures, particularly multilayer facades. Numerical results indicated a relationship between increased PCM thickness and resulting time lag. This relationship led to smoother indoor temperatures, with interior surface temperature rising closer to room temperature.

The aim of this study is to investigate the efficacy of PCMs in improving thermal comfort by increasing a building's inertia and stabilising indoor climates according to the National Construction Code (NCC) adopted in Australia [12]. To achieve this goal, a finite volume discretisation method is used within commercial package ANSYS Fluent to generate numerical results. The study utilise a model that replicates a building envelope with a macro-encapsulated PCM slab integrated into it. Macro-encapsulated PCM (Phase Change Material) refers to the integration of PCM into a composite at a macroscale level. In the context of macro-encapsulation in this work, the PCM is contained within a larger enclosure in a form of solid slab. The macro-encapsulation technique ensures that the PCM remains confined within the larger structure, preventing any leakage or direct contact with the surroundings. This slab allows for better control over the thermal behavior of the composite material, making it suitable thermal energy storage and transfer capabilities. This model is subjected to an averaged temperature during summer conditions in Sydney, Australia, to assess the PCM's effectiveness in a cooling passive technique. Specifically, a heat source is applied to a specific side of the envelope to simulate the heat of the sun. This allows the evaluation of the PCM's energy storage capacity and heat displacement under a summer-conditioned temperature gradient. The chosen PCM possesses appropriate thermophysical properties that align with the cooling passive technique requirements. In particular, the selected PCM has the solidification and melting properties that provide thermal comfort in building.

2. Problem Description

A building's envelope plays a crucial role in a building's inertia, capacity to ensure thermal comfort, and reduction of energy use and efficiency. The aim of this work is to demonstrate the practicality and effectiveness of utilizing phase change materials (PCMs) in a real-world building

envelope, providing insights into the feasibility of implementing this technology on a larger scale. The simulations conducted in this work compare two models adopted from 2022 National Construction Code (NCC) [12] and can be shown in Figure 1:

(a)

(b)
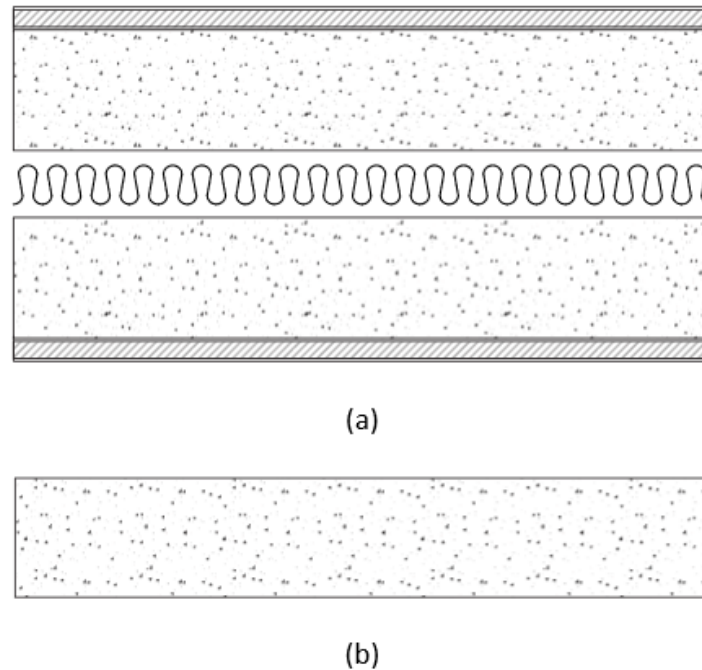
Figure 1 (a) A building envelope with a PCM component/layer where there are two leaves of 75 mm autoclaved aerated concrete wall panel; (b) A building envelope without the PCM addition where there is 125 mm thick concrete panel [12].

Figure 2 shows the geometry for the PCM geometry consists of three materials and 4 layers within the building envelope, concrete, PCM (RT22HC), concrete and plasterboard, respectively from left to right. The properties for RT22HC can be found in the data sheet provided from the supplier [13], with the concrete and plasterboard properties being displayed in Table 1.
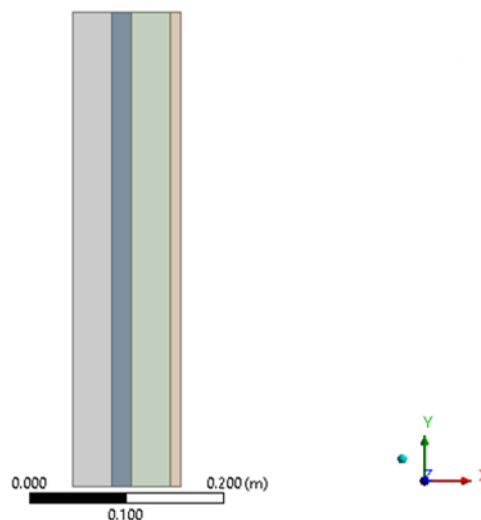
Figure 2 Geometry for 4-layered envelope; Concrete, PCM (RT22HC), concrete & plasterboard.

Table 1 Properties of solid materials used in building envelope.

Material	Density, $\rho\ (\frac{kg}{m^3})$	Specific Heat, $c_p\ (\frac{kJ}{kg \cdot K})$	Thermal Conductivity, $k\ (\frac{W}{m \cdot K})$
Concrete [14, 15]	2400	0.9	1.5
Plasterboard [16]	930	0.95	0.2

In the context of our study, "macro-encapsulated" signifies that the phase change material (PCM) is integrated into the composite layer at a macroscale level. To achieve this, we adopted an Eulerian approach, which allowed us to model and analyze the behavior of the PCM embedded within the concrete wall. The PCM layer, also referred to as a slab, is embedded within the concrete wall. Table 1 in the manuscript lists the distinct thermal properties of these two layers.

When selecting the most suitable phase change material (PCM) for each application, numerous factors must be considered. The most important consideration is the melting and solidus temperatures [17], as they govern the overall energy transfer rate to the storage system during charging and discharging [18]. The second priority after temperature is the PCM's latent heat (enthalpy of phase change), which maximizes the amount of energy stored throughout the phase transition [18]. Additionally, high latent heat allows for a high energy storage density, which is beneficial in applications where space is limited [18].

Thermal conductivity is also crucial when evaluating the thermophysical properties of PCMs, as different scenarios require different values depending on their specific use. One drawback of low thermal conductivity is the extended time required for charging or extracting energy within a reasonable timeframe [18]. However, for the chosen scenario of a building envelope, low thermal conductivity is preferred as it reduces heat transfer through the wall. Taking all these factors into account, the simulation selected RT22HC, an organic paraffin PCM manufactured by RubiTherm [13]. RT22HC is readily available off the shelf and can be ordered in bulk, making it ideal for a PCM slab. Organic PCMs have lower thermal conductivity while still maintaining excellent thermophysical properties, which is advantageous for heat transfer through a wall. Furthermore, RT22HC offers high thermal energy storage capacity, relatively constant heat storage and release temperatures at 22°C, no supercooling, chemical inertness, recyclability, and low thermal conductivity. These impressive thermophysical properties, combined with the fact that RT22HC does not contribute to CO2 emissions during the manufacturing process like inorganic PCMs, make it a suitable choice. Additionally, Sydney's average summer high temperature of 25.6°C aligns well with RT22HC's melting temperature, especially with the external protection provided by the first concrete layer [19]. The thermophysical properties of RT22HC can be found in Table 2.

Table 2 Thermophysical properties of RT22HC [13].

Melting Temp, $T_m\ (K)$	Enthalpy, $h\ (\frac{kJ}{kg})$	Specific Heat, $c_p\ (\frac{kJ}{kg \cdot K})$	Thermal Conductivity, $k\ (\frac{W}{m \cdot K})$	Density, $\rho\ (\frac{kg}{m^3})$	Viscosity, $\mu\ (\frac{Ns}{m^2})$
295.15 K	190	2	0.2	760	0.0257

For the simulation, the height of the envelope is set at 0.5 m, representing an isolated part of the wall with adiabatic boundaries to eliminate any interfering factors. The thickness of each component within the envelope is based on Figure 1(a) [12], consisting of two 40 mm concrete layers, a 20 mm PCM layer, and a 15 mm plasterboard layer. For the case without PCM, the geometry consists of 80 mm of concrete and a 15 mm plasterboard layer (refer to Figure 3).
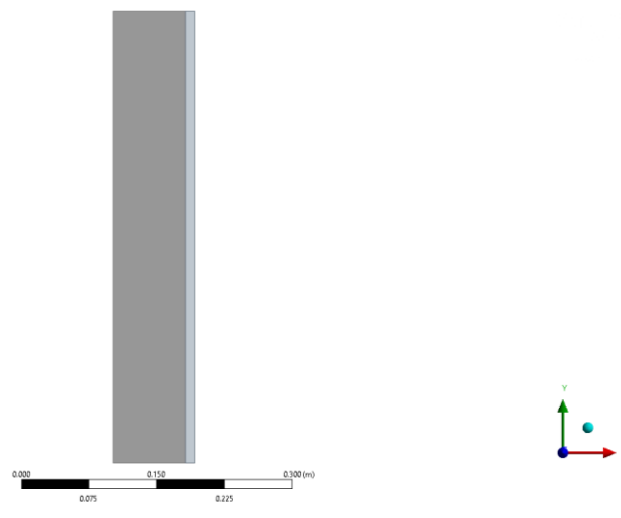
Figure 3 Geometry for 2-part envelope; Concrete & plasterboard.

3. Numerical Methodology

3.1 Governing Equation

The following governing equations describe the continuity, momentum and energy equations:
(I) Continuity equation

$$\nabla . V = 0 \tag{1}$$

(II) Momentum equation

$$\rho \left(\frac{\partial u_r}{\partial t} + V . \nabla u_r \right) = -\nabla P + \mu \nabla^2 u_r + \rho g \sin\theta + S_{u_r} \tag{2}$$

$$\rho \left(\frac{\partial u_\theta}{\partial t} + V . \nabla u_\theta \right) = -\nabla P + \mu \nabla^2 u_\theta + \rho g \cos\theta + S_{u_\theta} \tag{3}$$

(III) Energy equation

$$\frac{\partial}{\partial t}(\rho H) + \nabla . (\rho V H) = \nabla . (k \nabla T) \tag{4}$$

Where h and ΔH represent sensible enthalpy and latent heat, respectively ($H = h + \Delta H$). The term $\nabla . (\rho V H)$ is the transport of latent-heat evolution. Momentum sink is defined as:

$$S_{u_r} = -C(1-\lambda)^2 \frac{u_r}{\lambda^3 + \delta} \tag{5}$$

$$S_{u_\theta} = -C(1-\lambda)^2 \frac{u_\theta}{\lambda^3 + \delta} \tag{6}$$

Where, C is the mushy zone constant (set to 10^5 in this study). The enthalpy h is defined as:

$$h = h_{ref} + \int_{T_{ref}}^{T} C_p \, dT \tag{7}$$

Where, h_{ref} is the reference enthalpy at $(T_{ref} = 273 \, K)$. Melting heat is calculated based on latent heat L, i.e.:

$$\Delta H = \lambda L \tag{8}$$

λ denotes the liquid fraction of PCM during the solidification process, between the solidus and liquidus temperatures $(T_s < T < T_l)$:

$$\lambda = \begin{cases} 0, & T \leq T_s \\ \dfrac{T - T_s}{T_l - T_s} & T_s < T < T_l \\ 1, & T \geq T_l \end{cases} \tag{9}$$

To incorporate the natural convection motions within the liquid PCM and account for density variations, the Boussinesq approximation is employed. Consequently, the density of the liquid PCM can be represented as:

$$\rho = \frac{\rho_m}{\beta(T - T_m) + 1} \tag{10}$$

Where ρ_m indicates the original density of liquid PCM, β is the thermal expansion coefficient, and $T_m = (T_s + T_l)/2$. T_s and T_l are the solidus and liquidus temperatures, respectively.

3.2 Solution Approach

To ensure that the solution can be solved within a domain confidently, the domain must have strict initial and boundary conditions set, constraining the domain allowing a mathematical model to solve it accurately. Table 3 displays the chosen initial, boundary, and cell zone conditions.

Table 3 Initial, boundary and cell zone conditions.

Boundary/Initial/Cell Zone Conditions
Top and bottom walls: Adiabatic
Hot/left wall = 308.15 K
Cold/right wall = 293.15 K
Concrete-PCM (RT22HC) wall: Interface
PCM (RT22HC)-Concrete wall: Interface
Concrete-Plasterboard wall: Interface
Concrete Domains: Solid (Set Material: Concrete)
PCM Domain: Fluid (Set Material: RT22HC)

Plasterboard Domain: Solid (Set Material: Plasterboard)

To evaluate these conditions, the processing solver must be setup with the required means to solve the corresponding equations necessary to the prescribe scenario. This includes setting the solution method, solver technology, model, residuals and more. The selected variations for this simulation can be found in Table 4 for transient, gravity and 2D choices.

Table 4 Selected variables for preliminary simulation in ANSYS solver.

Selected Variables for ANSYS Fluent Solver	
General	Type: Pressure-Based
	Velocity Formulation: Absolute
	2D Space: Planar
	Time: Transient
	Gravity (On): Y = -9.81 m/s
Model	Solidification & Melting (On)
	Energy (On)
	Viscous - Laminar
Solution Methods & Controls	Scheme: SIMPLE
	Flux Type: Rhie-Chow - Momentum based
	Spatial Discretization:
	Gradient: Leash Squares Cell Based
	Pressure: Second Order
	Momentum: First Order Upwind
	Energy: First Order Upwind
Solution Controls	Momentum: 0.8
	Liquid fraction: 0.2
	Energy: 0.7
Monitors	Residuals:
	Continuity, X-Velocity, Y-Velocity: 1e-06
	Energy: 1e-09
Solution Initialisation	Initialisation Method: Standard
	Compute from: All zones
	Temperature: 293.15 K
Run Calculation	Type: Fixed
	Number of Time Steps: 60,000
	Time Steps Size: 0.5 s
	Max Iterations/Time Step: 30

A pressure-based SIMPLE scheme was chosen for its faster computation and lower memory requirements. Since the system consists only of convection with low velocities, there is no need for a density-based simulation.

To initiate the PCM phenomena, solidification and melting must be activated, requiring the inclusion of energy. The chosen residuals for convergence were set at 1e-06, with the energy

residual set at 1e-09. This level of accuracy ensures a precise representation of the phase change phenomena, with energy being the critical factor. The initial temperature for all zones was set at 293.15 K using standard initialization, guaranteeing consistent values throughout the system. The selected time step values ensured that the PCM transitioned completely before the end of the calculation, with smaller time steps enabling more accurate results.

3.3 Numerical Verification and Validation

In this section, the simulation method is validated by comparing it to the experimental findings of Al-Abidi et al. [20]. The initial and boundary conditions are determined based on the data reported in the reference study [20]. To perform this validation, a numerical examination of the phase change process of paraffin (RT82) is conducted in a triplex tube heat exchanger. The comparison plot in Figure 4 demonstrates a good agreement between the simulation and the experimental temperature data over a 65-minute period.
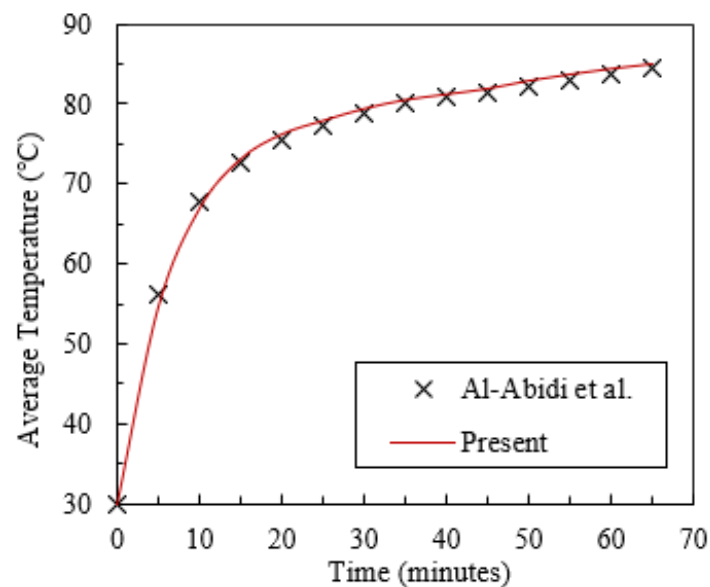
Figure 4 Validation against the experimental results [20].

The impact of mesh size and time-step on the numerical results is thoroughly investigated. Figure 5 illustrates the results of the grid independence analysis, where the transient liquid fraction is predicted for the dual-PCM configuration of case-6. Various numbers of cells ranging from 6000 to 22800 are examined in the numerical simulations, revealing that increasing the number of cells beyond 11900 does not significantly affect the predicted values of the liquid fraction. As a result, computational domains with 11900 cells are chosen for the predictions. The time step is also determined to be set at 0.1 s to ensure accurate predictions.
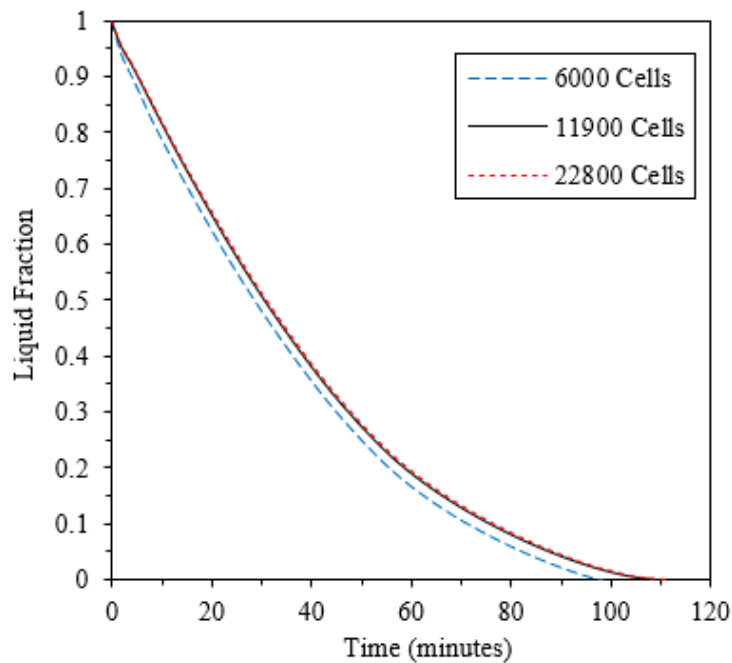
Figure 5 Mesh sensitivity test with different cells.

4. Results

This study employs a model that accurately replicates a building envelope incorporating a macro-encapsulated PCM slab. The analysis focuses on the PCM's energy storage capacity and heat displacement, specifically studying the time evolution of the melting processes. There is a steady increase in temperature and energy, with the mass fraction displaying contours very similar to those of the energy. This correlation is expected because the energy is directly linked to the mass fraction resulting from the melting of the PCM. It is evident that as the PCM melts, energy is stored within the fluid phase, representing a dischargeable sensible heat. This sensible heat will persist until the PCM cools down and solidifies again, releasing the heat back into the building either overnight or during a cool period.

4.1 Impact of PCM on Thermal Characteristics of Building Envelope

The temperature contours in the PCM-embedded simulation exhibit a consistent increase from the heat flux contact point until reaching the PCM (refer to Figures 6 (a-e)). Once the temperature reaches the PCM, there is a significant alteration in the heat transfer throughout the system due to differences in thermal conductivity and the energy required to melt the PCM. It can be observed that the PCM restricts conduction through itself into the other concrete leaf, thereby slowing down the heat transfer process across the envelope. At t = 1.5 hrs, the temperature of the concrete aligns with the melting pattern of the PCM. This pattern persists throughout the simulation, with the temperature gradient and heat transfer following the liquefaction of the PCM, resulting in reduced heat transfer through the recently liquefied sections. As a consequence, the temperature gradient traverses the building envelope from 75 s to 6 hrs.
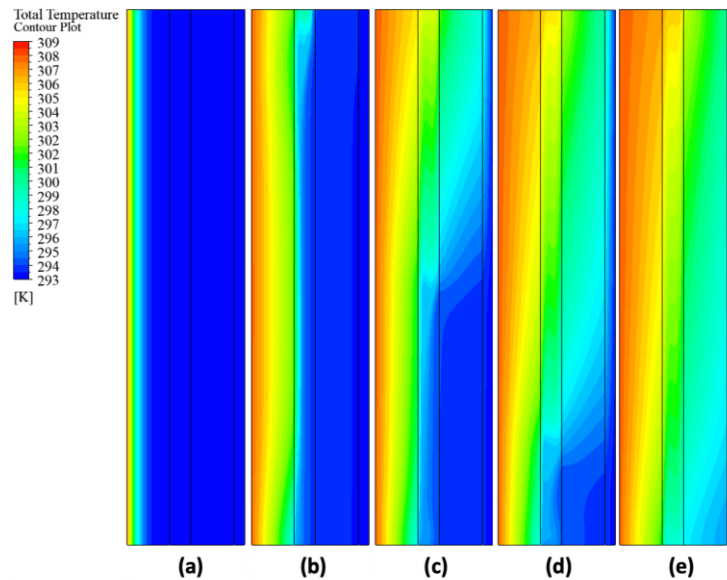
Figure 6 Temperature contour plots of PCM embedded building envelope: (a) 75 s (b) 1.5 hrs (c) 3 hrs (d) 4.5 hrs (e) 6 hrs.

This explanation highlights two key points. Firstly, heat transfer is more pronounced in the liquid form of the PCM, indicating that once the PCM is charged or in a liquid state, it exhibits enhanced convective properties. Secondly, the presence of the PCM promotes the occurrence of the buoyancy effect throughout its volume, consequently influencing the overall heat transfer across the building envelope. To illustrate these distinctions, Figure 7 presents temperature profiles at five different heights, each incrementing by 25% from the base of the model.
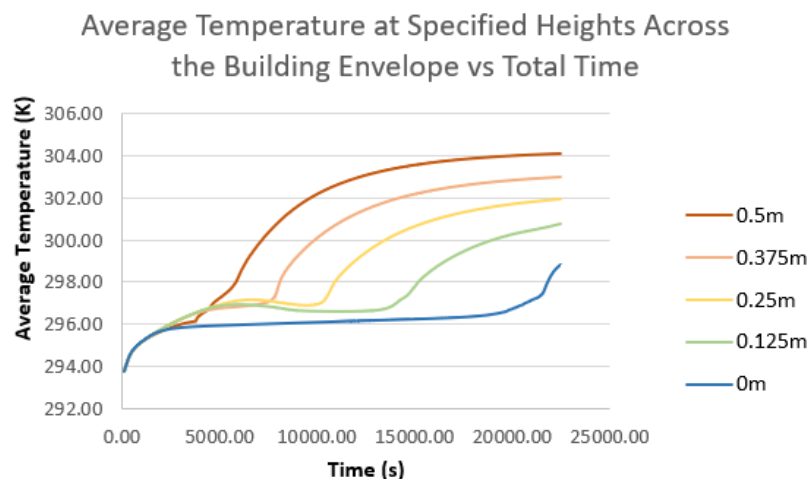
Figure 7 Average temperature versus time at different height of the PCM envelope.

Figure 7 clearly demonstrates the quantitative relationship between the average temperature across the building envelope and its corresponding height. Additionally, it provides insights into how the buoyancy effect within the PCM layer influences temperature dynamics throughout the simulation, specifically tied to the timing of phase changes. Notably, the temperatures steadily increase across all heights until 4000 s (slightly exceeding 1 hour), following which variations emerge.

This point marks the onset of distinctive temperature increases at different heights, each adhering to a logarithmic pattern attributed to the PCM's transition into a liquid state.

The logarithmic temperature patterns arising from the buoyancy effect become evident in Figure 7, showcasing the time disparities for temperature changes at varying heights. At the highest point (0.5 m), the logarithmic temperature increase commences at 6000 s (1.5 hrs), subsequently cascading to lower heights. The final logarithmic temperature increase begins at 15000 s (4 hrs) and propagates towards the base of the PCM. Consequently, the time differential for temperature change between the top and base of the PCM is approximately 15000 s.

Although temperatures vary, the trend exhibited in Figure 7 suggests that the scenario is approaching a quasi-steady state. It can be assumed that the temperature at 0m will also reach a quasi-steady state shortly after the PCM has completely melted at t = 6 hrs. Table 5 presents the results for the maximum, minimum, and average temperatures of the individual components within the building envelope. It is evident that the PCM reduces the overall heat transfer through the wall, as the second layer of concrete averages a temperature of 299.13 K and the plasterboard reaches a maximum of only 299.59 K.

Table 5 Temperature of each component within the PCM simulation after 6 hours.

Temperature of each component in the PCM embedded envelope				
Component	Concrete One	PCM RT22HC	Concrete Two	Plasterboard
Max. Temperature (K)	308.1	306.8	303.7	299.5
Min. Temperature (K)	301.3	297.0	295.4	293.2
Avg. Temperature (K)	306.4	302.6	299.1	295.5

Figures 8 (a-e) present the contour plots obtained from the second simulation, which focuses on the absence of PCM within the building envelope. In this simulation, the temperature contours exhibit a more conventional pattern of heat transfer across the wall, characterized by a structured and linear temperature gradient along the x-axis of the building envelope.
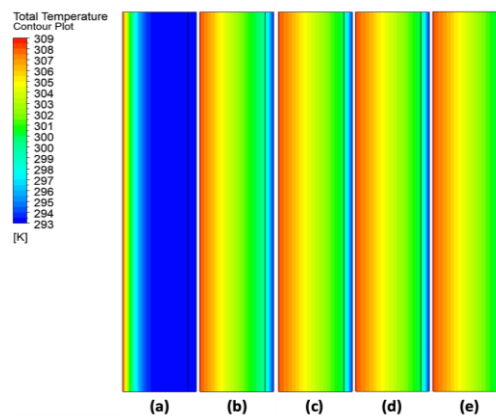
Figure 8 Temperature contour plots of non-PCM embedded building envelope: (a) 75 s (b) 1.5 hrs (c) 3 hrs (d) 4.5 hrs (e) 6 hrs.

An additional distinguishing aspect lies in the time needed for the system to achieve elevated temperatures across the building envelope. In the scenario without PCM, the system experiences a

rapid linear temperature rise, leading to the envelope reaching a temperature plateau after a mere 5000 s or 1 hour. This characteristic becomes apparent in the contour plots (as illustrated in Figures 8), depicting minimal temperature alterations after 1.5 hours, with only a marginal increase in temperature between 1.5 to 3 hours.

Conversely, in the non-PCM simulation, the system attains a quasi-steady state in a shorter duration. Around the 15000 s mark, the envelope enters a quasi-steady state, accompanied by a slight 0.01 K average temperature elevation during the last 7500 s. As anticipated, the absence of buoyancy effects, attributed to the lack of density variations and phase change transitions due to the absence of PCM, characterizes the scenario without PCM.

Table 6 presents the maximum, minimum, and average temperatures of each component in the simulation without PCM. Upon analysing the temperature data for each scenario, it becomes apparent that the building envelope with embedded PCM exhibits lower temperatures in all sections compared to the scenario without PCM. This is observed when comparing the singular concrete component to the combined temperatures of both concrete layers and the PCM layer. Additionally, the plasterboard registers lower maximum, minimum, and average temperatures, indicating that the PCM embedded wall reduces the amount of heat transferred into the building.

**Table 6** Temperature of each component within the non-PCM simulation after 6 hours.

Temperatures of each component in the envelope without PCM		
Component	Concrete	Plasterboard
Max. Temperature (K)	308.1	300.4
Min. Temperature (K)	300.5	293.2
Avg. Temperature (K)	304.3	296.8

However, the presence of the buoyancy effect within the PCM leads to higher temperatures at the top of the building envelope, which can be disadvantageous for those areas. The buoyancy effect causes heat to rise and gradually move towards the base of the envelope. This could result in the upper levels of a multi-story building experiencing faster temperature increases than the lower levels. To address this issue, the use of multiple PCMs on different floors could be considered, with longer melting times for upper floors and shorter melting times for lower floors. Ideally, the PCM should melt in a structured left-to-right fashion, ensuring that the temperature remains consistent across all floors of a building.

Overall, the PCM envelope brings about several positive impacts, including lower surface temperatures and reduced heat transfer, greatly enhancing the building's energy efficiency, thermal comfort, and durability. In addition to the overall temperature reduction, the increase in temperature within the envelope is advantageous as the PCM becomes charged and utilizes the heat to energize itself. This is in contrast to a standard envelope where excess heat is simply reduced, rejected, or left unused.

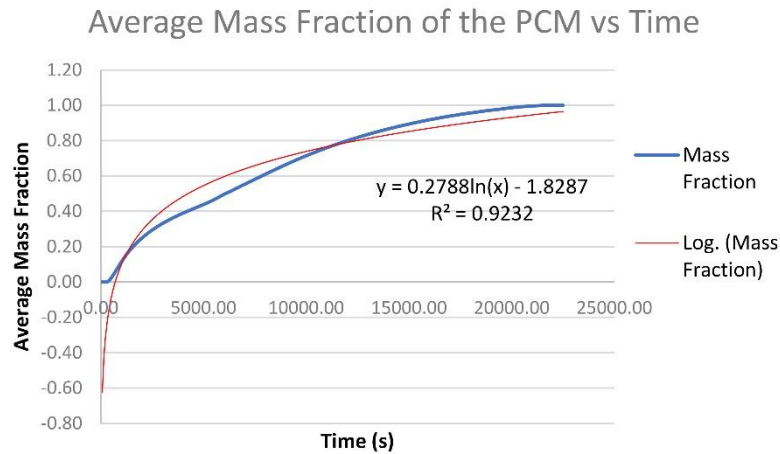### *4.2 Mass Fraction, Energy and the Buoyancy Effect*

Figures 9 (a)-(e) illustrate the change in mass fraction for the PCM embedded in the building. The mass fraction represents the composition of the fluid, with a value of 1.0 indicating a completely fluid state (represented by red), and a value of 0.0 representing a solid state (represented by blue). As the PCM undergoes its phase change from solid to liquid, there is a gradient transitioning from red to blue, with a semi-solid state displayed through a range of colors from orange to green. This color transition signifies the PCM's transformation from a solid to a liquid state, during which latent heat is stored between two sensibly heated zones.
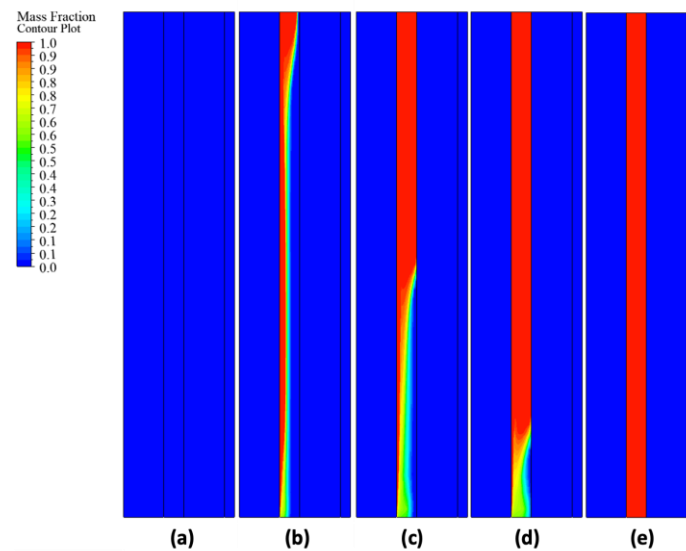
Figure 9 Mass Fraction contour plots of PCM embedded building envelope: (a) 75 s (b) 1.5 hrs (c) 3 hrs (d) 4.5 hrs (e) 6 hrs.

During the 0-1.5-hr timeframe, the PCM undergoes a phase change, leading to a change in its density. As a consequence, the liquid PCM, with a higher density, rises to the top of the solid PCM, creating a buoyancy effect driven by the density difference. This buoyancy effect results in an 'S'-shaped melting pattern, which significantly impacts the convective and conductive heat transfer within the building envelope. This behaviour can be observed as the 'storing profile' of the PCM. As time progresses, the buoyancy effect allows the PCM to gradually transition into a liquid state, following a downward trend as the PCM melts from the top to the bottom. Consequently, during the 3-6-hr timeframe, the bottom half of the PCM only melts once the PCM above it has completely melted.

The mass fraction plot, illustrated in Figure 10, clearly elucidates the non-uniform liquefaction process of the PCM over time. The initial melting rate exhibits rapid progression, gradually decelerating towards the final 30% of the remaining solid state. This slowdown is attributed to the diminishing temperature difference between the 4.5-hour to 6-hour period compared to the initial 0 to 1.5-hour period. Figure 10 showcases the average mass fraction of the PCM with respect to time. Within the first 7000 s (2 hours), the mass fraction index reaches 0.5, subsequently transitioning to a more gradual melting rate characterized by a logarithmic pattern. The complete liquefaction of the PCM occurs at 21000 s (6 hours).

Figure 10 Average Mass Fraction of the PCM against time.

Additionally, the buoyancy effect introduces a height dependency in the mass fraction analysis of the system. It is not possible to analyze the mass fraction of the PCM at a single height since the mass fraction varies with height. By plotting the mass fraction at different heights of the PCM against time, it becomes evident that the time taken for the PCM to melt increases as the height decreases. Figure 11 illustrates the time required for the PCM to melt at various heights.
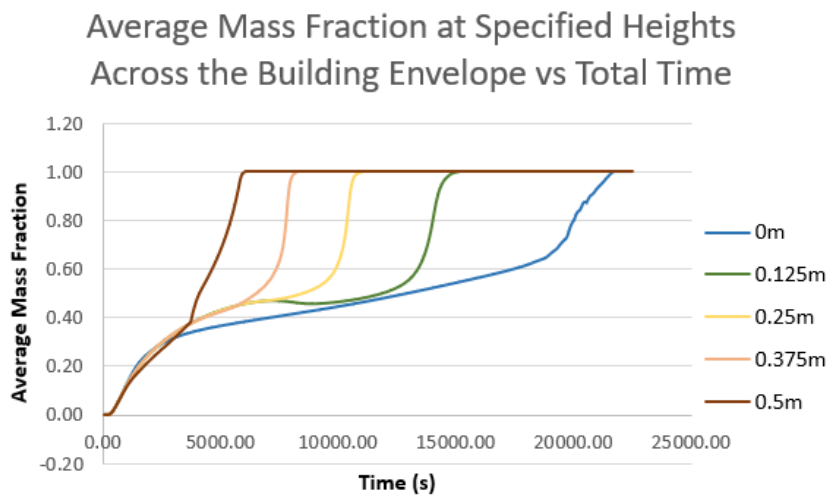

Figure 11 Average Mass Fraction at different heights against time.

At a height of 0.5 m, the PCM undergoes liquefaction in a linear manner, attaining a mass fraction of 1.0 by 6250 s (1.7 hours). In contrast to the lower heights, the complete liquefaction process occurs more rapidly. For instance, at 0.375 m, full liquefaction is reached after 8400 s, while at 0.25 m it occurs at 11500 s, at 0.125 m it occurs at 16000 s, and at the base of the PCM (0 m), complete melting transpires at 21850 s. As such, the time disparity for liquefaction between the highest and lowest points of the PCM is approximately 16000 s. This disparity underscores the profound influence of the buoyancy effect on the melting dynamics of PCM within an envelope.

Significantly, this top-down melting trend holds substantial implications for the building's inertia at various heights, owing to alterations in thermal resistances and diminished heat transfer at lower

elevations. Furthermore, Figure 7 and Figure 11 establish a discernible correlation between height and temperature, underscoring the prominent role played by the buoyancy effect.

When comparing the energy and mass fraction contour plots, a clear correlation is observed between the storing profile/mass fraction and the energy contour plot, indicating the storage of energy as sensible heat. This correlation is evident in Figures 12 (a)-(e), where the plots exhibit identical patterns throughout the entire simulation, with the energy contour plot reflecting the same patterns as the mass fraction plots.
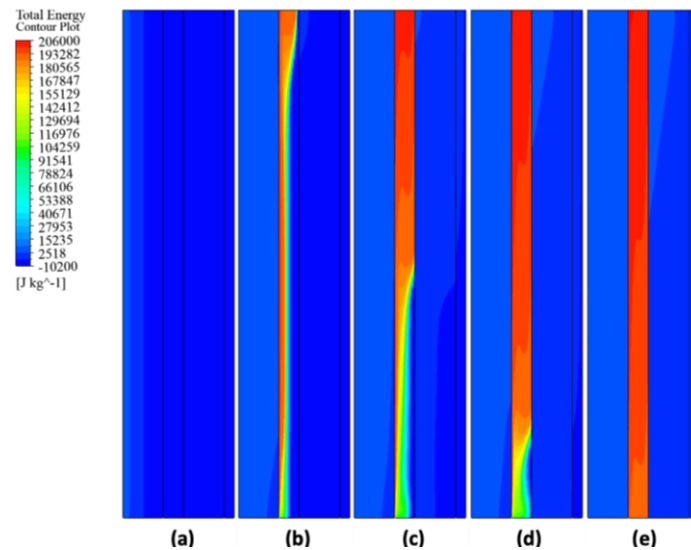
Figure 12 Energy contour plots of PCM embedded building envelope: (a) 75 s (b) 1.5 hrs (c) 3 hrs (d) 4.5 hrs (e) 6 hrs.

Figure 13 provides a visual representation of how the average energy varies at specific heights along the building envelope over time. These energy profiles correspond to the mass fraction data shown in Figure 11, demonstrating that as the phase change material (PCM) undergoes melting, the absorbed energy rises. Notably, the rate of heat storage is more pronounced at greater heights within the structure. By the 21850 s, the entire PCM has melted, resulting in a peak average energy of 200 kJ/kg.
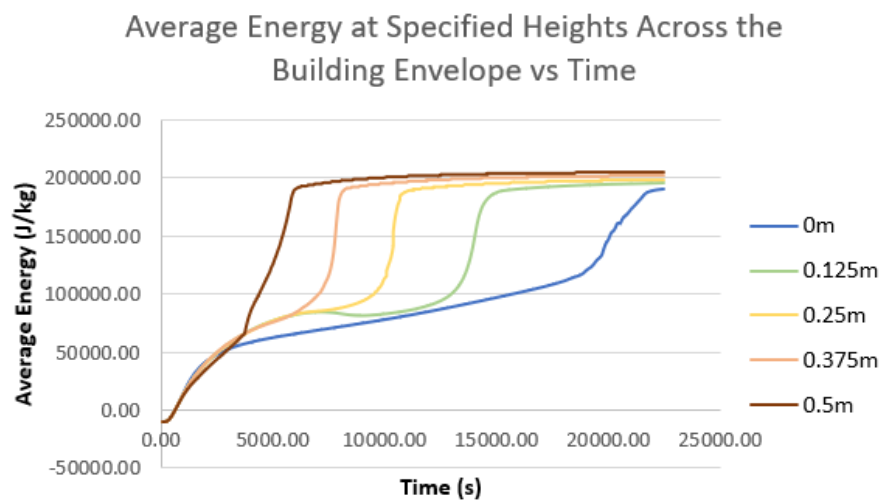
Figure 13 Average Energy at different heights against time for the PCM simulation.

The correlation between energy and mass fraction is significant due to the storage of enthalpy during the phase change of the PCM, which is manifested as energy. This relationship is particularly evident when comparing the mass fraction plot with the energy plot, as depicted in Figure 10 & Figure 14. The patterns observed in both the height-specific mass fraction plot and the overall average energy plot over time are remarkably similar, further reinforcing this correlation.
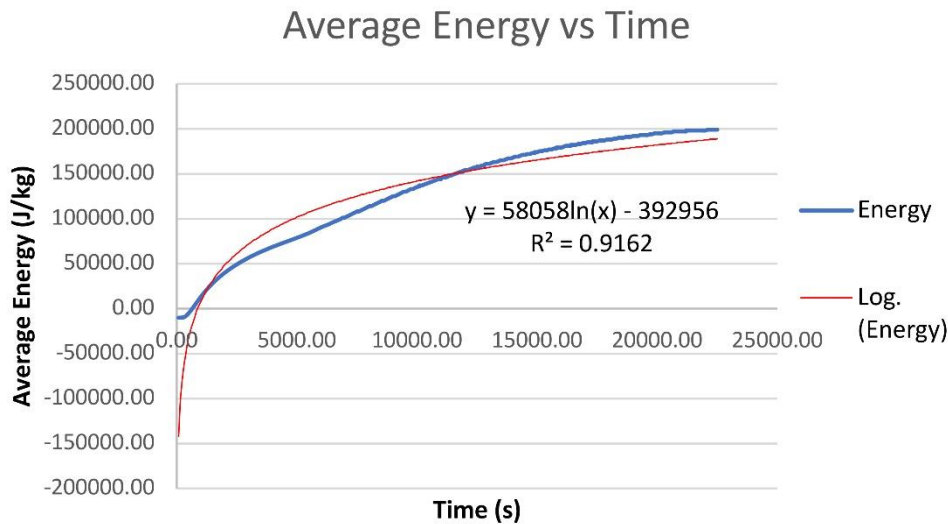
Figure 14 Average Energy against time for the PCM simulation.

This correlation demonstrates the effectiveness of the PCM, which serves two passive functions. Firstly, it acts as a heat sink, absorbing and reducing the heat transmitted through the envelope via convection and conduction. Secondly, it stores this absorbed energy, which can be later utilized once the surrounding heat flux has dissipated. It is worth noting that once the PCM has melted, the internal energy within the liquid areas reaches 206 kJ and gradually spreads throughout the PCM as it undergoes phase transitions over time. This energy represents readily available sensible heat, which can be released when the surrounding temperature gradient drops below its critical point (22 degrees). In essence, the PCM effectively utilizes both ends of the temperature spectrum, absorbing heat while in the solid state and releasing heat while in the liquid state, thanks to its latent heat properties and high storage capacity. This significantly improves the efficiency of buildings compared to those without PCM, where heat either dissipates with wasted energy or is transferred into the building, requiring additional energy to achieve desirable levels of thermal comfort.

This is applicable in the second scenario where no PCM is present within the envelope. In this scenario, the temperature exhibits a linear increase without any buoyancy effect. As depicted in Figures 15 (a-e), the energy follows a similar linear pattern, traversing the building envelope in the x-direction at a much slower rate compared to the PCM scenario. The energy in this simulation shows minimal variations throughout the entire duration, with only slight incremental changes observed from t = 75 s to t = 3 hrs. This is evident in the contour plots (refer to Figures 15), where the energy exhibits minimal colour changes. The reason behind this is that the concrete in this scenario does not retain the transferred heat like the PCM does. Consequently, the energy peaks in this scenario only reach 8.7 kJ at the final 6-hour mark.
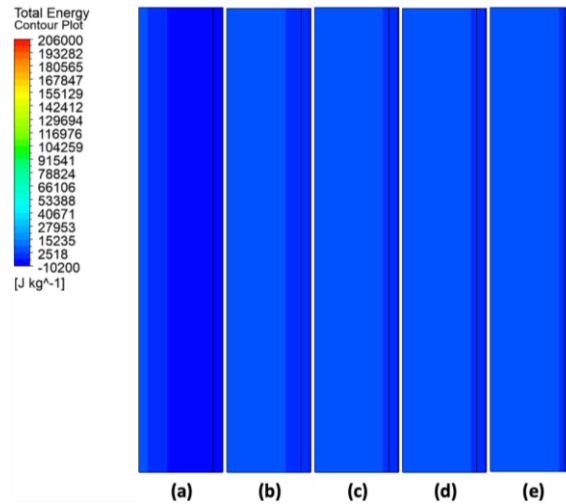
Figure 15 Energy contour plots of non-PCM embedded building envelope: (a) 75 s (b) 1.5 hrs (c) 3 hrs (d) 4.5 hrs (e) 6 hrs.

This implies that the increase in temperature and heat transfer entering the building in this scenario are essentially irrelevant, negatively impacting the building's performance. Therefore, the non-PCM envelope necessitates higher energy consumption to maintain cooling during the day, and potentially additional energy demand for heating during the night. In contrast, the heat absorbed by the PCM is stored as energy, enhancing the building's thermal inertia and reducing power consumption. This leads to lower overall power usage during peak periods throughout the day, thanks to reduced heat transfer, as well as decreased energy consumption at night due to the release of stored heat back into the building.

4.3 Entropy

The contour plots in Figures 16 (a-e) display the entropy at different time instants, showing the changes in entropy and the phenomena of the PCM as it undergoes phase transitions at different temperatures.
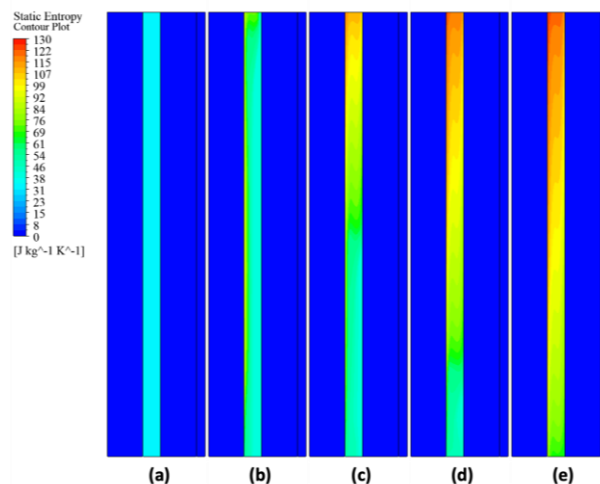
Figure 16 Entropy contour plots of PCM embedded building envelope at different time instant (a) 75 s (b) 1.5 hrs (c) 3 hrs (d) 4.5 hrs (e) 6 hrs.

At t = 0 s, when the PCM exists in its solid state, it exhibits a low level of entropy, indicating a high degree of order and predictability, with entropy values uniformly distributed around approximately 40 J/kg·K. As time advances, the PCM initiates the melting process, resulting in a subsequent rise in entropy. Within the molten section of the PCM, higher entropy values signify a greater degree of disorder compared to the solid portion, which exhibits a declining gradient of entropy. This observation highlights the system's dependency on temperature and mass fraction for its level of disorder. As the system's temperature rises, the PCM progressively melts, absorbing energy and transitioning into a liquid state. This phenomenon stems from the rapid melting of the PCM, which escalates the molecular disorder, leading to an increase in entropy. In an ideal scenario, as the PCM's temperature drops below its solidus temperature, the molecules gradually decelerate as the PCM solidifies, causing entropy to decrease toward zero. Notably, the entropy plots of the PCM offer valuable insights into the system's behavior during state transitions. This evaluative information holds potential for the design and optimization of energy storage systems employing PCM, particularly in applications like thermal energy storage for buildings. At t = 6 hrs, specific entropy measurements illustrate the transition: the upper portion of the PCM exhibits an entropy of 130 J/kg·K, which is three times greater than its solid state, while the lower segment records 60 J/kg·K, marking a doubling of the initial value. This differentiation signifies the profound impact of the melting process on the system's entropy distribution, revealing the extent of molecular disorder at different levels within the PCM.

5. Discussion

In conclusion, the integration of Phase Change Materials (PCMs) within building envelopes offers a compelling quantitative framework for enhancing energy efficiency, thermal comfort, and overall durability. Through their ability to absorb and store heat energy during phase change, PCMs effectively curtail heat transfer through convection and conduction. This inherent passive behavior contributes to lowered surface temperatures and significantly reduces the need for supplemental energy consumption in cooling or heating processes.

The analysis of temperature profiles, mass fraction plots, and energy contour plots has revealed the significant impact of the buoyancy effect and the melting pattern of the PCM on heat transfer within the envelope. The melting process, occurring from top to bottom, influences thermal resistances and results in a non-uniform liquefaction process. This behavior highlights the importance of carefully considering the height-dependent characteristics of the PCM when implementing it in multi-story buildings.

Comparisons between the PCM-embedded envelope and the scenario without PCM demonstrate the clear advantages of PCM implementation. The PCM envelope exhibits lower temperatures in all sections, reduced heat transfer, and improved thermal performance compared to the non-PCM scenario. The PCM effectively utilizes the energy absorbed during its solid state and releases it when the surrounding temperature gradient decreases, further contributing to energy efficiency. Remarkably, the Phase Change Material (PCM) accomplishes 50% of its average melting process in the initial 2-hour period, followed by a gradual deceleration in the rate of melting. Subsequently, it takes approximately 6 hours for the PCM to undergo complete liquefaction. As the PCM undergoes the melting process, the system's entropy values experience a discernible increase, reflecting an augmentation in disorder. Notably, at the uppermost section of the building, the

entropy value reaches 130 K/kg·K, signifying an expansion of more than threefold compared to the initial value.

The convergence of mass fraction and energy contour plots underscores the direct correlation between PCM storage profile and energy distribution within the envelope. The capacity of PCMs to store energy as sensible heat significantly bolsters their role as a robust thermal management solution. Quantitatively, the analysis of entropy values reveals substantial shifts during the melting process. At t = 6 hrs, the top of the PCM records 130 J/kg·K, which is three times more than the solid state, while the bottom part registers 60 J/kg·K, doubling the solid state value of 40 J/kg·K.

Overall, the findings support the use of PCM in building envelopes as a means to optimize energy consumption, enhance thermal comfort, and increase the building's durability. Importantly, the geometry of the simulation is based on the national construction code, ensuring that this study provides a real representative of current building structures and practices. As the analyses underscore the importance of these nuanced aspects, careful consideration of height-dependent melting patterns and thermal resistances is paramount to ensure optimal performance and efficiency. The advent of PCM technology in building design holds immense promise for fostering sustainable and energy-efficient construction practices, driven by a quantitatively informed understanding of their dynamic impact.

Potential future research directions stemming from this study encompass the exploration of PCM-integrated envelopes within dynamic environmental conditions. This encompasses variations in external temperature and solar radiation, which would yield a more authentic evaluation of their efficacy and adaptability. Given the current study's focus on summer conditions, undertaking climate-specific investigations becomes particularly pertinent.

Author Contributions

Conceptualization, A.L. and D.D.L.; methodology, A.L and Z.B.; software, Z.B.; investigation, Z.B.; data curation, Z.B.; writing—original draft preparation, Z.B.; writing—review and editing, A.L and D.D.L.; supervision, A.L. and D.D.L.

Competing Interests

The authors have declared that no competing interests exist.

References

1. Bueno AM, de Paula Xavier AA, Broday EE. Evaluating the connection between thermal comfort and productivity in buildings: A systematic literature review. Buildings. 2021; 11: 244.
2. HVAC HESS. Guide to Best Practice Maintenance and Operation of HVAC systems for Energy Efficiency [Internet]. Canberra, Australia: Department of Climate Change and Energy Efficiency; 2022. Available from: http://energycut.com.au/business/wp-content/uploads/2015/02/HVAC-Best-Practice-Guide.pdf.
3. Al Yasiri Q, Szabó M. Incorporation of phase change materials into building envelope for thermal comfort and energy saving: A comprehensive analysis. J Build Eng. 2021; 36: 102122.
4. Aridi R, Yehya A. Review on the sustainability of phase-change materials used in buildings. Energy Convers Manage. 2022; 15: 100237.

5. Wang N, Adeli H. Sustainable building design. J Civ Eng Manage. 2014; 20: 1-10.

6. Geng D, Yang X, Li D, Yang R, Ma Y, Wu Y, et al. Numerical investigation of photothermal performance of glazed window integrated with airflow channel and phase change material. Energy Sources Part A. 2023; 45: 8203-8217.

7. Faraj K, Khaled M, Faraj J, Hachem F, Castelain C. Phase change material thermal energy storage systems for cooling applications in buildings: A review. Renew Sustain Energy Rev. 2020; 119: 109579.

8. Tyagi VV, Buddhi DP. PCM thermal storage in buildings: A state of art. Renew Sustain Energy Rev. 2007; 11: 1146-1166.

9. Yang X, Li D, Yang R, Ma Y, Tong X, Wu Y, Arıcı M. Comprehensive performance evaluation of double-glazed windows containing hybrid nanoparticle-enhanced phase change material. Appl Therm Eng. 2023; 233: 119976.

10. Uludaş MÇ, Tuncbilek E, Yıldız Ç, Arıcı M, Li D, Krajčík M. PCM-enhanced sunspace for energy efficiency and CO_2 mitigation in a house in mediterranean climate. J Build Eng. 2022; 57: 104856.

11. Liu C, Zhang G, Arıcı M, Bian J, Li D. Thermal performance of non-ventilated multilayer glazing facades filled with phase change material. Sol Energy. 2019; 177: 464-470.

12. National Construction Code. National Construction Code 2022 [Internet]. Canberra, Australia: Australian Building Codes Board; 2023. Available from: https://ncc.abcb.gov.au/editions/ncc-2022.

13. RUBITHERM. RT22HC Data Sheet [Internet]. Berlin, Germany: Rubitherm Technologies; 2020. Available from: https://www.rubitherm.eu/media/products/datasheets/Techdata_-RT22HC_EN_09102020.PDF.

14. Dorf RC. The engineering handbook 2nd Edition. The Electrical Engineering Handbook. Boca Raton: CRC press; 2005.

15. Yang IH, Park J, Kim KC, Yoo SW. A comparative study on the thermal conductivity of concrete with coal bottom ash under different drying conditions. Adv Civ Eng. 2021; 2021: 7449298.

16. Rusthi M, Keerthan P, Ariyanayagam A, Mahendran M. Numerical studies of gypsum plasterboard and MgO board lined LSF walls exposed to fire. Proceeding of International Conference on Performance-based and Life-cycle Structural Engineering; 2015 December 9-11; Brisbane, QLD, Australia. Brisbane, QLD, Australia: School of Civil Engineering, The University of Queensland.

17. Department of Energy, USA. Quadrennial Technology Review [Internet]. Washington, USA: Department of Energy; 2022. Available from: https://www.energy.gov/sites/prod/files/2017/03/f34/qtr-2015-chapter5.pdf.

18. Noël JA, Kahwaji S, Desgrosseilliers L, Groulx D, White MA. Phase change materials. In: Storing Energy. Amsterdam, Netherlands: Elsevier; 2022. pp. 503-535.

19. Bureau of Meteorology. Climate statistics for Australian locations [Internet]. Canberra, Australia: Commonwealth of Australia; 2022. Available from: http://www.bom.gov.au/climate/averages/tables/cw_066062.shtml.

20. Al Abidi AA, Mat S, Sopian K, Sulaiman MY, Mohammad AT. Experimental study of melting and solidification of PCM in a triplex tube heat exchanger with fins. Energy Build. 2014; 68: 33-41.